Protein Science (1997), 6:89–98. Cambridge University Press. Printed in the USA.

Importance of the release of strand 1C to the polymerization mechanism of inhibitory serpins

WUN-SHAING W. CHANG, JAMES WHISSTOCK, PAUL C.R. HOPKINS,[1] ARTHUR M. LESK, ROBIN W. CARRELL, AND MARK R. WARDELL[2]

Department of Haematology, University of Cambridge, MRC Centre, Hills Road, Cambridge, CB2 2QH, United Kingdom

(RECEIVED September 4, 1996; ACCEPTED October 23, 1996)

Abstract

Serpin polymerization is the underlying cause of several diseases, including thromboembolism, emphysema, liver cirrhosis, and angioedema. Understanding the structure of the polymers and the mechanism of polymerization is necessary to support rational design of therapeutic agents. Here we show that polymerization of antithrombin is sensitive to the addition of synthetic peptides that interact with the structure. A 12-mer peptide (homologous to P_{14}-P_3 of antithrombin reactive loop), representing the entire length of s4A, prevented polymerization totally. A 6-mer peptide (homologous to P_{14}-P_9 of antithrombin) not only allowed polymerization to occur, but induced it. This effect could be blocked by the addition of a 5-mer peptide with the s1C sequence of antithrombin or by an unrelated peptide representing residues 26–31 of cholecystokinin. The s1C or cholecystokinin peptide alone was unable to form a complex with native antithrombin. Moreover, an active antitrypsin double mutant, Pro 361 → Cys, Ser 283 → Cys, was engineered for the purpose of forming a disulfide bond between s1C and s2C to prevent movement of s1C. This mutant was resistant to polymerization if the disulfide bridge was intact, but, under reducing conditions, it regained the potential to polymerize. We have also modeled long-chain serpin polymers with acceptable stereochemistry using two previously proposed loop-A-sheet and loop-C-sheet polymerization mechanisms and have shown both to be sterically feasible, as are "mixed" linear polymers. We therefore conclude that the release of strand 1C must be an element of the mechanism of serpin polymerization.

Keywords: antithrombin; antitrypsin; inhibitor; modeling; peptide; polymerization; protein dysfunction; serpin

Mammalian blood plasma contains members of the serpin superfamily of serine proteinase inhibitors, which function as important regulators of the coagulation, inflammation, fibrinolysis, and complement cascades (for reviews see Travis & Salvesen, 1983; Gettins et al., 1993; Potempa et al., 1994). Crystal structures have shown that they share a highly conserved tertiary fold consisting of three large β-sheets surrounded by nine α-helices (Loebermann et al., 1984; Baumann et al., 1991; Mourey et al., 1993), and a loop containing the reactive scissile bond, denoted P_1-P_1' (Schechter & Berger, 1967), which interacts with cognate proteinases (Huber & Carrell, 1989).

One of the most striking features of the serpins is their dramatic conformational rearrangement. For example, when inhibitory serpins are cleaved at their P_1-P_1' bond, the N-terminal residues of the reactive loop form a new strand within the A-sheet, accompanied by an increase in structural stability (Loebermann et al., 1984; Baumann et al., 1991, 1992; Mourey et al., 1993). This conformational change is believed to be crucial for serpin inhibitory function (Gettins et al., 1993). Serpins are also known to polymerize, with consequences of clinical importance. Several natural variants, such as antithrombin Rouen VI (Asn 187 → Asp) (Bruce et al., 1994); the Z (Glu 342 → Lys) (Lomas et al., 1992), S_{iiyama} (Ser 53 → Phe) (Lomas et al., 1993b), and M_{malton} (Phe 52 deleted) (Lomas et al., 1995) variants of antitrypsin; α_1-antichymotrypsin (Pro 229 → Ala) (Faber et al., 1993) and C1-inhibitor mutants (Ala 436 → Thr, Val 451 → Met, Pro 476 → Ser, Phe 455 → Ser) (Aulak et al., 1993; Eldering et al., 1995) have been shown to polymerize spontaneously, resulting in thromboembolism, emphysema, liver cirrhosis, and angioedema. Native inhibitory serpins were also found to undergo this noncovalent polymerization after limited thermal denaturation or mild treatment with denaturants, such as guanidine hydrochloride (Mikus et al., 1993; Lomas et al., 1995; Patston et al., 1995).

Proposed mechanisms of serpin polymerization involve the interaction of the reactive loop of one molecule with either the A- or

Reprint requests to: Wun-Shaing Wayne Chang, Department of Haematology, University of Cambridge, MRC Centre, Hills Road, Cambridge CB2 2QH, UK; e-mail: wsc11@cus.cam.ac.uk.

[1]Present address: Gladstone Institute of Cardiovascular Disease, University of California San Francisco, P.O. Box 419100, San Francisco, California 94141-9100.

[2]Present address: Department of Biochemistry and Molecular Biophysics, Washington University School of Medicine, 660 South Euclid Avenue, Box 8231, St. Louis, Missouri 63110-1093.

C-sheet of another molecule (Fig. 1). The "loop-A-sheet polymerization mechanism" suggests that inactive polymers are formed by the insertion of a portion of the reactive loop of a molecule (approximately residues P_8-P_3) into the A-sheet of another molecule and so on. Support for this model comes from the observation that incubation of inhibitory serpins with synthetic peptides homologous to their reactive loops results in serpin/peptide binary complexes with thermostability properties similar to the cleaved species (Schulze et al., 1990; Björk et al., 1992). It is assumed that such peptides insert into the A-sheet of the serpin molecule like the reactive loop of the cleaved form (Schulze et al., 1990; Björk et al., 1992). Moreover, cleavage of antitrypsin at the P_9-P_8 or P_{10}-P_9 bond results in spontaneous polymerization (Mast et al., 1992), suggesting that the P_{15}-P_9 or P_{15}-P_{10} region inserts into the top of the A-sheet leaving the bottom of the A-sheet open and allowing the P_8-P_3 or P_9-P_3 region of another molecule to insert. This loop-A-sheet polymerization mechanism is also consistent with the recently solved structure of an intact functional recombinant antitrypsin (Elliott et al., 1996) in which the P_8-P_3 is in the necessary β-pleated strand conformation for reactive loop insertion.

Previously, the dimeric crystal structure of antithrombin revealed another possible mechanism of serpin polymerization (Carrell et al., 1994). The antithrombin crystal structure contains a dimer in which the reactive loop of one molecule in the native active state inserts into the C-sheet of a second molecule in the latent inactive conformation (Carrell et al., 1994). Based on this observation, it was suggested that serpin polymers form by the reactive loop of each acceptor molecule first inserting into its own A-sheet to liberate strand 1C (s1C) from its own C-sheet, which can then be replaced by the loop of a donor molecule (Carrell et al., 1994; Lomas et al., 1995; Stein & Carrell, 1995). This is the "loop-C-sheet polymerization mechanism."

Here we report experiments using antithrombin and antitrypsin to investigate the mechanism of serpin polymerization. These include the use of synthetic peptides to induce and block polymerization, and molecular modeling to examine and verify the stereochemical feasibility of possible mechanisms. We have constructed an active antitrypsin double mutant (denoted S–S antitrypsin) in which Pro 361 and Ser 283 were each replaced with cysteine to form a disulfide bridge to prevent movement of s1C. These results suggest the necessity for the release of s1C from the C-sheet during serpin polymerization. Our modeling studies indicate that this would be a common feature of both loop-A-sheet and loop-C-sheet mechanisms of polymer formation.

Results

Induction of serpin polymerization by synthetic peptide

The interaction of serpin molecules with synthetic peptides was investigated by incubating native antithrombin with a 100-fold molar excess of various peptides at 37 °C for several days. Aliquots taken at different incubation times were run on nondenaturing PAGE, where the antithrombin/peptide complexes migrate more anodally than the free inhibitors due to acquisition of additional negative charges contributed by the incorporated acetylated peptides (Schulze et al., 1990). Figure 2A shows that, in the absence of any peptide, the electrophoretic properties of native antithrombin were not altered by prolonged incubation at 37 °C. As shown previously (Chang et al., 1996), a 12-mer peptide homologous to the reactive loop of antithrombin (residues P_{14}-P_3) formed a binary complex with antithrombin and totally prevented polymerization (Fig. 2B). However, we were surprised to find that a 6-mer peptide corresponding to the P_{14}-P_9 segment of antithrombin not only permitted polymerization, but induced it (Fig. 2C).

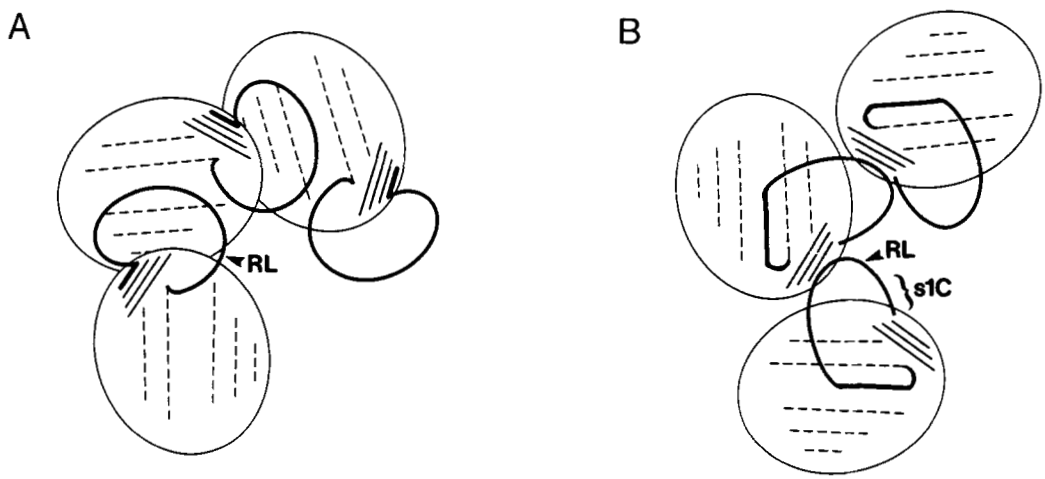

Fig. 1. Schematic representation of the loop-A-sheet and the loop-C-sheet models of the mechanism of serpin polymerization. The common feature of both models is the opening of the A-sheet, which will then allow the reactive loop to insert into the gap. **A:** The loop-A-sheet model. Serpin polymerization occurs by the reactive loop of one molecule inserting into the A-sheet of another molecule to build up polymers. **B:** The loop-C-sheet model. Serpin polymers are formed by the loop of each acceptor molecule first inserting into its own A-sheet enough to liberate its strand 1C from the C-sheet; the space in the C-sheet then becomes occupied by the reactive loop of a donor molecule. Bold solid lines denote the reactive loop (RL) and dashed lines indicate the five strands of the A-sheet of the inhibitor. In the loop-A-sheet model, four strands of the C-sheet were shown with the s1C (solid line) linked to the C terminus of the reactive loop, whereas, in the loop-C-sheet model, the s1C is displaced, leaving the C-sheet with one less strand.

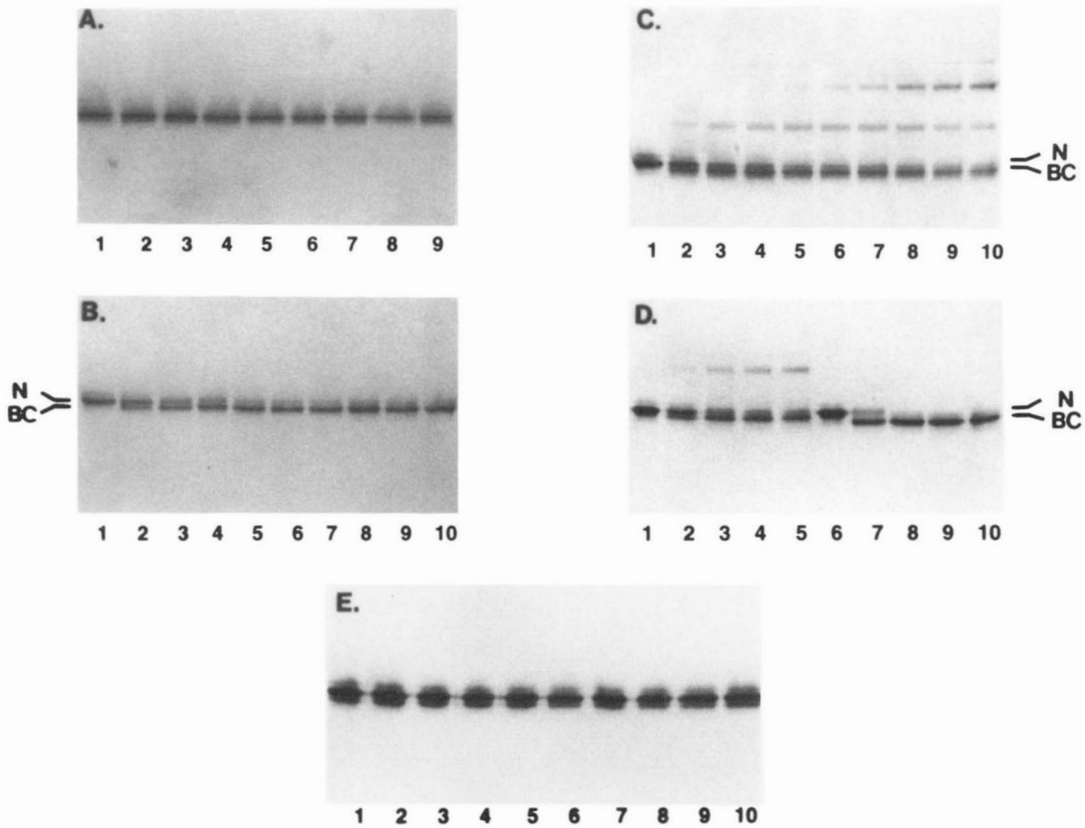

Fig. 2. Nondenaturing gradient PAGE (7.5–15% w/v acrylamide) of the interaction of antithrombin with synthetic peptides. All the peptides were incubated with native antithrombin at a peptide:serpin molar ratio of 100:1 at 37 °C for the times indicated. **A:** Lanes 1–9 represent aliquots of the control native antithrombin incubated alone for 0, 6, 12, 24, 48, 60, 72, 84, and 96 h, respectively. **B:** Lanes 1–10 represent aliquots of native antithrombin incubated with the synthetic reactive-loop 12-mer peptide (P_{14}-P_3 of antithrombin) for 0, 2, 4, 6, 8, 10, 12, 18, 24, and 48 h, respectively. **C:** The incubation time was as for B, except that antithrombin was incubated with the reactive-loop 6-mer peptide (P_{14}-P_9 of antithrombin). **D:** Lanes 1–5 represent samples removed from the incubation reaction of native antithrombin with both its reactive-loop 6-mer peptide and s1C 5-mer peptide (TFKAN) together at 0, 12, 24, 48, and 72 h, respectively. Lanes 6–10 represent samples removed from the incubation reaction of native antithrombin with both its reactive-loop 6-mer peptide and the cholecystokinin 6-mer peptide (residues 26–31 of cholecystokinin Ac-DYMGWM) at 0, 12, 24, 48, and 72 h, respectively. **E:** Lanes 1 and 10, control native antithrombin; lanes 2 and 3 represent samples removed from the incubation reaction of native antithrombin with s1C 5-mer peptide at 0 and 48 h, respectively; lanes 4 and 5 represent samples of native antithrombin incubated with the 5-mer peptide (sequence 5–9 of rat prothrombin precursor FLEEI) for the same time points; lanes 6 and 7 correspond to samples of the incubation of antithrombin with the cholecystokinin 6-mer peptide for 0 and 48 h, respectively; lanes 8 and 9 were as for lanes 2–3, but with antithrombin incubated with the 13-mer peptide (sequence of human mini gastrin I Ac-LEEEEEAYGWMDF). N, native antithrombin; BC, antithrombin/peptide binary complexes.

Blockage of serpin polymerization by synthetic peptides

Polymerization of antithrombin was induced using the synthetic 6-mer peptide (residues P_{14}-P_9 of antithrombin reactive loop). It was reasoned that, if the release of s1C is important to the polymerization mechanism, a peptide homologous to s1C of antithrombin (TFKAN) may inhibit such polymerization. As shown in Figure 2D (lanes 1–5), the addition of s1C 5-mer peptide as well as the reactive-loop 6-mer peptide did indeed block polymerization by predominately forming antithrombin/peptide binary complexes with only a small fraction of dimeric antithrombin. Surprisingly, as shown in Figure 2D (lanes 6–10), the addition of the unrelated 6-mer peptide from the sequence of cholecystokinin (Ac-DYM GWM) as well as the antithrombin reactive-loop 6-mer peptide not only inhibited antithrombin polymerization, but also resulted in 100% antithrombin/peptide binary complex formation. Using this method, we could not determine which peptide(s) was associated with the antithrombin/peptide binary complexes. We assume that it was the antithrombin reactive-loop 6-mer peptide because this did form some binary complexes with more anodal migration on the gel when added alone to antithrombin (Fig. 2C). No such change in electrophoretic migration was observed for antithrombin incubated with its own s1C 5-mer peptide or cholecystokinin 6-mer peptide alone (Fig. 2E, lanes 2–3, 6–7). Neither the control synthetic 5-mer peptide, representing the sequence 5–9 of rat prothrombin precursor (FLEEI), nor the 13-mer peptide from the sequence of human mini gastrin I (Ac-LEEEEEAYGWMDF) was able to form binary complexes with antithrombin (Fig. 2E) or to inhibit its polymerization (data not shown).

Characterization of the Pro 361 → Cys, Ser 283 → Cys antitrypsin double mutant

In an attempt to discriminate further between the two possible mechanisms of serpin polymerization, we constructed an antitrypsin variant in which two cysteines were introduced into positions

that would favor the formation of a disulfide bond between s1C and s2C to prevent the release of s1C. The stoichiometries of inhibition of human leukocyte elastase by both the reduced and oxidized forms of this S–S antitrypsin mutant were shown to be the same as native antitrypsin, and their association rate (K_{ass}) was affected only slightly (P.C.R. Hopkins, W.-S.W. Chang, M.R. Wardell, and S.R. Stone, unpubl. obs.). The desired disulfide bond between the Cys 361 and Cys 283 positions of the oxidized S–S antitrypsin mutant was confirmed both by Ellman assay and amino acid analysis, showing that a total of three cysteines were present, but that, in the absence of reducing reagents, only one available sulfhydryl group was measured (data not shown). Limited proteolysis also confirmed the existence of this disulfide bond: papain normally cleaves native antitrypsin at the P_7-P_6 and P_1-P_1' bonds (Mast et al., 1992) and results in an increased mobility of antitrypsin on SDS-PAGE due to the release of a ~4-kDa C-terminal fragment from the molecule (Fig. 3, lanes 1–6). Such cleavage analyses on the S–S antitrypsin mutant showed that approximately 60–70% of the cleaved C-terminal fragment was still bound to the molecule through the newly formed S–S bridge and resulted in no electrophoretic shift on SDS-PAGE under nonreducing conditions (Fig. 3, lanes 9–10). However, breaking the disulfide bond of this cleaved material by incubation with a reducing reagent such as DTT (DL-dithiothreitol) at 23 °C for 4 h prior to electrophoresis produced an electrophoretic shift identical to that of cleaved wild-type antitrypsin (Fig. 3, lanes 12–13).

The thermostability of the S–S antitrypsin mutant was compared with that of plasma and recombinant wild-type antitrypsins. All antitrypsins were heated at 56 °C for the time indicated in Figure 4, followed by centrifugation for 15 min at 20,000 × *g* and deceleration without braking. A small fraction of each supernatant was subjected to nondenaturing PAGE and electron microscopy. On incubation at 56 °C, both plasma and recombinant wild-type antitrypsins undergo polymerization. In contrast, the S–S antitrypsin mutant demonstrated a much increased thermostability that allowed it to retain its monomeric conformation at this temperature (Fig. 4). By breaking the disulfide bond of the mutant through the addition of reducing reagent prior to heat treatment, the increased thermostability of this reduced S–S antitrypsin was lost, and the S–S antitrypsin underwent polymerization readily (Fig. 4). However, unlike those heat-induced polymers of plasma serpins (Lomas et al., 1992; Bruce et al., 1994), electron microscopy of the reduced recombinant S–S antitrypsin showed that the size of the polymers are large and the shapes of these polymers are highly diverse, and therefore could not be observed by nondenaturing PAGE as easily as the polymers of plasma native antitrypsin (Fig. 4).

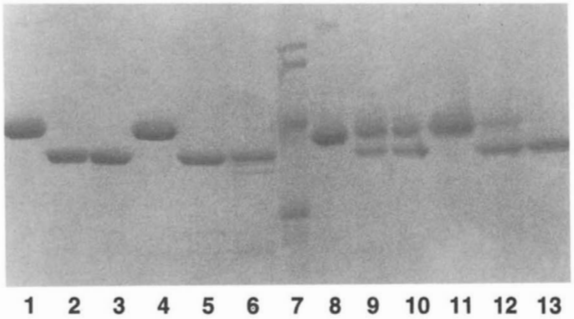

Fig. 3. Limited proteolysis of recombinant wild-type and S–S antitrypsins by papain. All the cleavage reactions were performed at 37 °C for 2 h with the final concentration of protein being 0.25 mg/mL. The proteins were examined on 10–20% (w/v) SDS-PAGE. Lane 1, recombinant wild-type antitrypsin; lanes 2 and 3, samples removed from the cleavage reaction of wild-type antitrypsin with papain at a serpin:proteinase ratio of 250:1 and 100:1 (w:w), respectively; lane 4–6, as for lanes 1–3, except that the samples removed from the cleavage reaction of wild-type antitrypsin with papain were first heated at 100 °C for 2 min and then incubated in 100 mM DTT at 23 °C for 4 h prior to electrophoresis; lane 7, molecular weight marker (four major bands from top to bottom: 77, 67, 43, 30 kDa); lane 8, recombinant S–S antitrypsin mutant; lanes 9 and 10, samples removed from the cleavage reaction of the S–S antitrypsin with papain at a serpin:proteinase ratio of 250:1 and 100:1 (w:w), respectively; lane 11–13, as for lanes 8–10, except that the samples removed from the cleavage reaction of S–S antitrypsin with papain were first heated at 100 °C for 2 min and then incubated in 100 mM DTT at 23 °C for 4 h prior to electrophoresis.

Modeling of serpin polymers: Structures of the models

In the antithrombin loop-C-sheet polymerization model, the insertion of the reactive loop of a molecule into its own A-sheet is only to P_{14} (data not shown), but it is possible for the reactive loop to insert further into the A-sheet and maintain correct stereochemistry with hydrogen bonding of the loop of one molecule to s2C of another. This is seen in the antitrypsin models, which have insertion to P_{12}. As a model of the loop-C-sheet dimer of antitrypsin shows (Fig. 5A), some hydrogen bonds were formed in the C-sheet region between s2C of molecule A and reactive loop residues P_5-P_1 of molecule B. There are also hydrogen bonds between the H-helix of molecule A and the F-helix of molecule B (Fig. 5A). An antitrypsin loop-C-sheet pentamer is also shown in Figure 5B, demonstrating that we are able to form long-chain polymers with our loop-C-sheet model. However, because electron micrographs of polymers show them to be of different shapes and sizes (Fig. 4), there is likely to be some deviation in the relative orientation of the monomers. Therefore, contacts and hydrogen bonding between the monomers will vary.

In our model of serpin loop-A-sheet polymers, the P_8-P_3 region of one molecule is inserted into the A-sheet of another molecule in the same anti-parallel fashion as seen in the cleaved structure (Loebermann et al., 1984; Baumann et al., 1991, 1992; Mourey et al., 1993). As a model of the loop-A-sheet dimer of antitrypsin shows (Fig. 6A), the reactive loop of both molecules was designed to adopt an ovalbumin-like turn at the top of the A-sheet with s1C being partially peeled off in order to allow formation of long-chain polymers to occur. Moreover, some β-sheet hydrogen bonds are formed between reactive loop residues P_8-P_3 of molecule B and A-sheet strands 3A and 5A of molecule A (Fig. 6A). Again, because electron micrographs of polymers show them to be of different shapes and sizes (Fig. 4), some deviation in the relative orientation of the monomers and the subsequent contacts and hydrogen bonding between the monomers will probably take place. However, from our loop-A-sheet models of antitrypsin polymers (Fig. 6B) and antithrombin polymers (data not shown), we show that flexibility in s1C is required so that long-chain polymers can form without steric hindrance. The flexibility of the regions (P_9-P_{15} and P_1'-P_5') connecting to residues P_8 and P_1 could account for the variability in the shape of the polymers.

Modeling of serpin polymers: Quality of the models

The final CHARMm energies of both the loop-C-sheet and loop-A-sheet polymerization models were negative (i.e., −43,540 kcal/mol for the antitrypsin loop-C-sheet polymerization model and

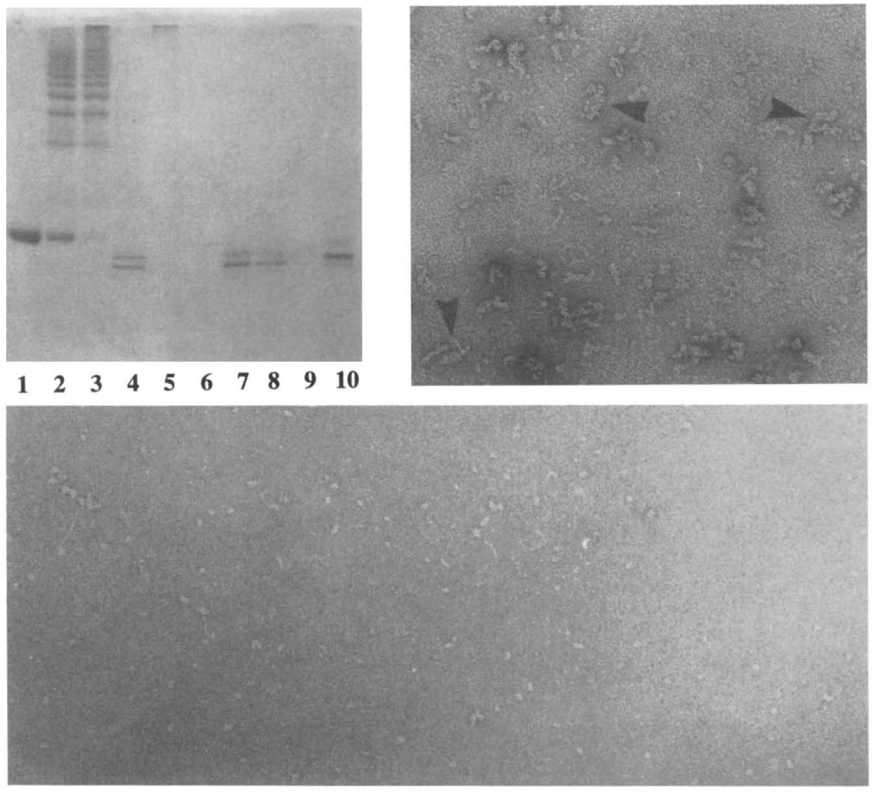

Fig. 4. Heat stability of antitrypsin assayed by nondenaturing gradient PAGE (7.5–15% w/v acrylamide) and electron microscopy. Top left: lane 1, plasma native antitrypsin; lanes 2 and 3, plasma antitrypsin heated at 56 °C for 30 and 60 min, respectively; lane 4, oxidized recombinant wild-type antitrypsin; lane 5, oxidized recombinant wild-type antitrypsin heated at 56 °C for 30 min; lane 6, reduced recombinant wild-type antitrypsin heated at 56 °C for 30 min; lane 7, oxidized recombinant S–S antitrypsin; lane 8, oxidized S–S antitrypsin heated at 56 °C for 120 min; lane 9, reduced S–S antitrypsin heated at 56 °C for 30 min; lane 10, reduced recombinant S–S antitrypsin. Bottom: electron micrograph of the oxidized S–S antitrypsins incubated at 56 °C for 60 min. Top right: electron micrograph of the reduced S–S antitrypsin incubated at 56 °C for 15 min (some polymers indicated by arrows). All preparations were negatively stained with uranyl acetate and viewed at a magnification of 123,000.

−42,432 kcal/mol for the antitrypsin loop-A-sheet polymerization model), indicating that there were no serious steric clashes. In both models, the ϕ, ψ, and ω angles of the reactive loop were checked and found to be satisfactory (i.e., within 20 °C of allowed conformations in a Ramachandran plot).

Discussion

Several natural serpin variants have been demonstrated to polymerize spontaneously at pyrexial temperatures, which consequently lowers the amount of active circulating serpin, resulting in severe clinical disorders (Lomas et al., 1992, 1993a, 1995; Faber et al., 1993; Bruce et al., 1994; Eldering et al., 1995). The best studied is the Z variant of antitrypsin, where the Glu 342 → Lys mutation is thought to disrupt the top of the A-sheet (Wu & Foreman, 1990; Lomas et al., 1993a). Other variants have also provided evidence that molecular distortions altering the distance between strands 3A and 5A of the A-sheet may play an important role in the mechanism of serpin polymerization (Aulak et al., 1993; Bruce et al., 1994).

There are data suggesting that the Z variant (Glu 342 → Lys) of antitrypsin polymerizes via the loop-A-sheet mechanism (Lomas et al., 1992) and that the antitrypsin M_{malton} (Phe 52 deleted) mutation causes polymerization by the loop-C-sheet mechanism (Lomas et al. 1995). Koloczek et al. (1996) recently have shown by fluorescence measurements that an essential part of the mechanism of polymerization is the mobility of s1C. Our models of polymers support this finding and suggest that s1C would need to be completely released in both the loop-C-sheet and loop-A-sheet polymerization models. This is also consistent with the observation that serpin mutations within s1C, such as the Val → Met mutation at the P'_8 residue of C1-inhibitor (Eldering et al., 1995), polymerize spontaneously. Mutations destabilizing s1C and adjacent regions would lead to greater mobility of the reactive loop, and consequently increase the likelihood of polymerization occurring.

The S–S antitrypsin mutant effectively provides a disulfide bond between s1C and s2C (Figs. 3, 4). This disulfide bond would either inhibit loop-C-sheet polymerization by preventing the displacement of s1C or stop loop-A-sheet polymerization by reducing the mobility of the reactive loop. Our models have shown that to prevent steric clashes in the formation of long-chain loop-A-sheet polymers, it is important to have mobility both in s1C and in the P_{16}-P_8 region of the reactive loop (Fig. 6A).

The observation that polymerization is induced by a synthetic antithrombin reactive-loop 6-mer peptide (Fig. 2C) affords alternative approaches to investigation of the mechanism of polymerization. One explanation for this effect could be that the 6-mer peptide inserts into the top of the A-sheet, leaving the bottom half

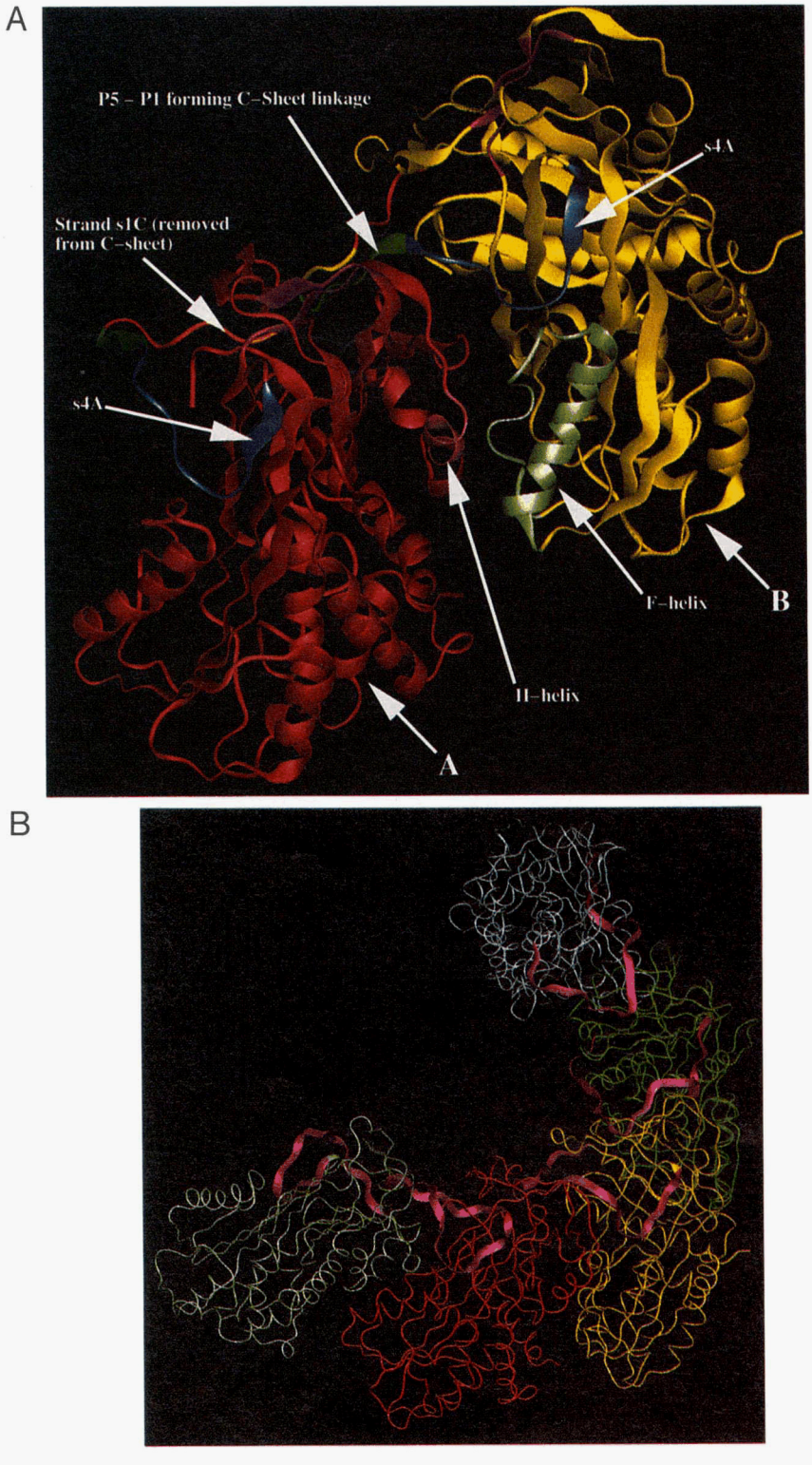

Fig. 5. A: Model of a loop-C-sheet dimer of antitrypsin. The two molecules, A and B, are shown in red and yellow, respectively. Strands 2C and 3C are purple and residues P_5-P_1 (which form the interaction with the C-sheet in the dimer) are green. Strand 1C (which is pulled out) is orange and the turn out of the A-sheet is blue. The F-helix of molecule B is light green and the H-helix of molecule A is pink. **B:** Model of an antitrypsin loop-C-sheet pentamer with each molecule colored differently. The reactive loop is shown in purple in each monomer.

of the A-sheet open and able to receive the reactive loop from another molecule to form loop-A-sheet polymers. Alternatively, the insertion of the 6-mer peptide into the A-sheet could disrupt the reactive-loop conformation and strand 1C leading to the formation of loop-C-sheet polymers. Hence, the capacity of the antithrombin s1C peptide to inhibit polymerization induced by the reactive-loop 6-mer peptide (80% blockage, Fig. 2D, lanes 1–5) may be best explained by its binding to the site left vacant by the displacement of the intact s1C strand, preventing further binding of the reactive loop of other molecules to form loop-C-sheet polymers. It is more difficult to foresee a mechanism whereby the s1C peptide inhibits loop-A-sheet polymerization. However, we believe that the s1C

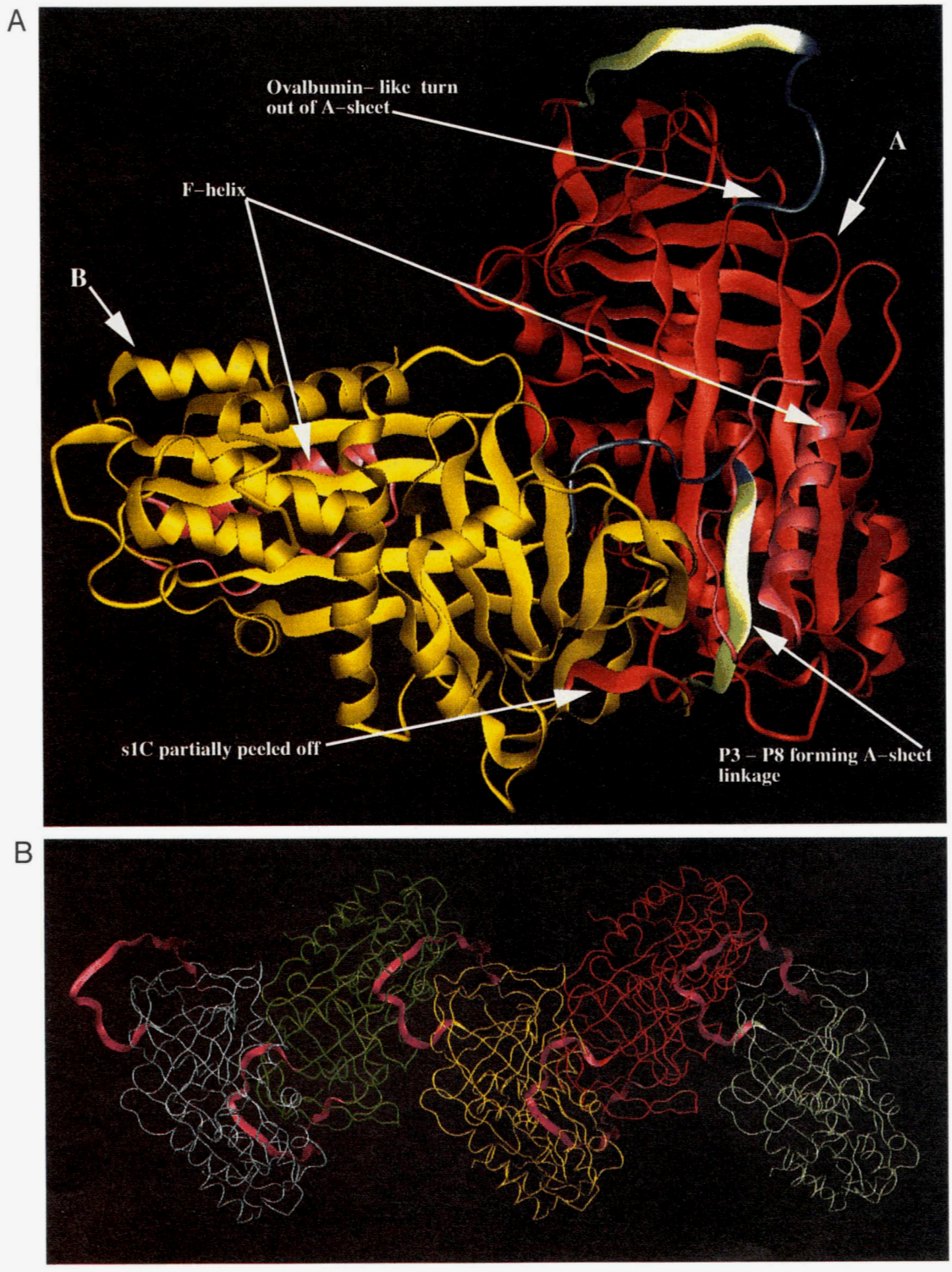

Fig. 6. A: Model of a loop-A-sheet dimer of antitrypsin. The two molecules, A and B, are shown in red and yellow, respectively. In both monomers, the turn at the top of the A-sheet is blue and s1C (which is pulled out) is orange. The F-helix is pink and residues P_8-P_3 are green. **B:** Model of an antitrypsin loop-A-sheet pentamer with each molecule colored differently. The reactive loop is shown in purple in each monomer.

peptide may be binding in such a way that it reduces the mobility of the reactive loop and subsequently hinders the loop-A-sheet polymer formation.

In this study, the synthetic 5-mer peptide from the sequence 5–9 of rat prothrombin precursor FLEEI, the 6-mer peptide representing residues 26–31 of cholecystokinin Ac-DYMGWM and the 13-mer peptide from the sequence of human mini gastrin I Ac-LEEEEEAYGWMDF were each obtained for use as controls for several reasons: (1) they were of similar size to those representing various regions of antithrombin; (2) they would not be expected to

be able to enter the A-sheet of serpin molecules because they contained contiguous large bulky-chained amino acids; (3) if they did form binary complexes with serpin molecules, they would alter the electrophoretic mobility by adding net charge to the complexes. As shown in Figure 2E, these peptides alone were unable to form a complex with native antithrombin. Surprisingly, unlike two other control peptides, the unrelated cholecystokinin peptide was able to block the polymerization (100% blockage, Fig. 2D, lanes 6–10) induced by the reactive-loop 6-mer peptide. Nevertheless, due to the relatively slow speed of serpin/peptide binary complex formation, neither the s1C peptide nor the cholecystokinin peptide is capable of blocking the rapid polymerization induced by heat treatment at 60 °C (data not shown). Because these data do not distinguish between the two mechanisms of polymerization, we speculate that the synthetic cholecystokinin peptide causes blockage of serpin polymerization in a similar way to that seen with the antithrombin s1C peptide. We are currently conducting crystallization trials on antithrombin complexed with its reactive-loop 6-mer peptide and the cholecystokinin 6-mer peptide to determine where these peptides bind and how a cholecystokinin peptide can block serpin polymerization so effectively. This should also indicate the mechanism of polymerization induced by the reactive-loop 6-mer peptide.

In conclusion, the properties of the active S–S antitrypsin mutant indicate the importance of mobility in the s1C region during polymerization. The disulfide mutant also provides other potential applications, such as preventing native plasminogen activator inhibitor-1 from undergoing the transition to the inactive latent form. Moreover, S–S mutations at similar positions in other serpins could be used to increase stability and subsequently facilitate the crystallization of the active conformation. The mechanism of serpin polymerization is complex. Our data is compatible with both the loop-C-sheet and loop-A-sheet models, supporting the finding of Koloczek et al. (1996) that both mechanisms of serpin polymerization may coexist.

Materials and methods

Materials

Unless otherwise stated, all reagents and enzymes were obtained from either BDH Chemicals Ltd. (Bristol, UK) or Sigma Chemical Co. (Dorset, UK). Heterogeneous porcine heparin was obtained from Grampian Enzymes (Arthrath, Scotland, UK). Human α-thrombin was a gift of Dr. Jean-Marie Freyssinet (Université Louis Pasteur Strasbourg, Institut d'Hématologie et d'Immunologie, Strasbourg, France). Leukocyte elastase was kindly provided by Dr. Stuart Stone (Department of Haematology, University of Cambridge, UK). *Escherichia coli* $BL21_{(DE3)}$ was supplied by Dr. F. William Studier (Brookhaven National Laboratories, Upton, New York). Rifampicin was obtained as Rifadin® from Merion Merrell Dow Ltd. (Uxbridge, UK).

Purification of plasma native antithrombin and antitrypsin

Antithrombin was purified from 2 L of fresh frozen plasma using heterogeneous heparin-Sepharose as published previously (McKay, 1981; Chang et al., 1996). Antitrypsin was isolated from 200 mL of fresh frozen plasma from an M homozygote as detailed previously (Lomas et al., 1993a). All the protein concentrations were determined by an A_{280} measurement using an extinction coefficient for 1% solution of 6.5 for antithrombin (Nordenman et al., 1977) and 5.4 for antitrypsin (Travis & Johnson, 1981). The proteins were snap frozen in liquid N_2 and stored at −80 °C until use. Prior to each experiment, the specific activities of the purified antithrombin and antitrypsin were checked to ensure that they were more than 70% active against human α-thrombin and bovine α-chymotrypsin, respectively (Lomas et al., 1993a; Bruce et al., 1994).

Production of recombinant wild-type and Pro 361 → Cys, Ser 283 → Cys antitrypsins

Recombinant wild-type antitrypsin and the Pro 361 → Cys, Ser 283 → Cys mutant (S–S antitrypsin) were produced in *E. coli* $BL21_{(DE3)}$ under the control of the T7 RNA polymerase promoter using the vector pΔN15 as described previously (Hopkins & Stone, 1995). The S–S antitrypsin mutant was made by PCR, exploiting the *Ava* I restriction site that lies at a position corresponding to the codons for residues 362 and 363, and the *Bst* XI site that lies upstream of residue 283. The Pro 361 → Cys oligonucleotide used was GAACTTGAC**CTCGGGG**CAGATAGACATGGG, in which the mutation is underlined and the *Ava* I restriction site is in bold. The Ser 283 → Cys oligonucleotide used was CGATATCATCA **CCAAGTTCCTGG**AAAATGAAGACAGAAGGTGTGCCAG CTTAC, in which the mutation is underlined and the *Bst* XI restriction site is in bold. PCR was performed with these two oligonucleotides and the product was cut with *Bst* XI and *Ava* I and then cloned into pΔN15 that was cut with the same two enzymes. Hence, the wild-type fragment was removed and replaced with a fragment containing the double mutation Pro 361 → Cys and Ser 283 → Cys. The entire region amplified by PCR was sequenced to ensure the presence of the desired mutation and the absence of any Taq-induced error.

E. coli $BL21_{(DE3)}$ was transformed with pΔN15 containing the S–S antitrypsin cDNA. Two 2-L flasks, each containing 1 L of 2xTY media, were inoculated with 10 mL of an overnight culture of transformed *E. coli* and grown with shaking at 37 °C. When the OD at 600 nm reached 0.6, IPTG was then added to a final concentration of 100 μg/mL. After 30 min, rifampicin dissolved in DMSO (100 mg/mL) was added to a final concentration of 100 μg/mL and the culture grown for a further 3 h until harvesting by centrifugation. The pellet was stored at −80 °C until the purification was performed. The S–S antitrypsin mutant was purified from inclusion bodies. Cells (10 g) were resuspended in 30 mL of 300 mM NaCl, 50 mM Tris, 10 mM EDTA, 0.5% Triton X-100, pH 8.0, and were lysed by three passages through a French press. Inclusion bodies and cellular debris were collected by centrifugation at 5,000 × g for 20 min, the pellet was resuspended in 30 mL of the above buffer, vortexed vigorously, and centrifuged again. This procedure was repeated three times to wash the inclusion bodies, which were then dissolved in 10 mL of 8 M guanidine hydrochloride, 100 mM DTT, 50 mM Tris, pH 8.0. Following purging by N_2, the solution was incubated at 50 °C for 2 h. The S–S antitrypsin was refolded by direct dropwise dilution into 1.6 L of N_2-purged 5 mM DTT, 50 mM Tris, pH 8.0, at room temperature. The refolded mutant was loaded directly onto a 50 mL Q-sepharose column equilibrated in N_2-purged 50 mM NaCl, 5 mM DTT, 50 mM Tris, pH 8.0, at 4 °C, and the bound proteins were eluted using a 200-mL linear gradient of 50–250 mM NaCl. All buffers were N_2-purged. The S–S antitrypsin eluted at ~150 mM NaCl. After purity was checked by SDS-PAGE, the mutant-containing fractions were purged with N_2 and stored at −80 °C. The S–S bond was allowed to form by removal of DTT by dialysis overnight against 5 L of 50 mM NaCl, 50 mM Tris, pH 8.0,

with three changes. Amino acid analysis of the S–S antitrypsin mutant was performed by the Department of Biochemistry, University of Cambridge, UK, and the Ellman assay, performed to determine the total and available sulfhydryl of the S–S antitrypsin, was done as published previously (Ellman, 1959).

PAGE

SDS-PAGE was performed using 10–20% (w/v) linear gradient gels according to the method of Laemmli (1970), but using 2-amino-2-methyl-1,3-propanediol instead of Tris base. Nondenaturing PAGE was a modification of the method of Goldenberg (1989) and was performed using 7.5–15% (w/v) linear gradient gels, with 53 mM Tris, 68 mM glycine, pH 8.9, as the cathode buffer, and 100 mM Tris-HCl, pH 7.8, as the anode buffer (Bruce et al., 1994). In both gel systems, 4–5 μg of protein was loaded in each lane.

Peptide annealing experiments

The synthetic 12-mer Ac-SEAAASTAVVIA, 6-mer Ac-SEAAAS, and 5-mer TFKAN peptides representing, respectively, the reactive loop P_{14}-P_3, P_{14}-P_9, and s1C sequences (P'_8-P'_{12}) of antithrombin were prepared by the Department of Biochemistry, University of Cambridge, UK, on an Applied Biosystems (California) peptide synthesizer. The synthetic peptides were purified by reverse-phase HPLC on a C-18 column with a 30–50% (v/v) acetonitrile gradient in 50 mM ammonium acetate, verified, and quantitated by amino acid composition analysis and Edman degradation. The synthetic 5-mer peptide from the sequence 5–9 of rat prothrombin precursor FLEEI, the 6-mer peptide representing residues 26–31 of cholecystokinin Ac-DYMGWM, and the 13-mer peptide from the sequence of human mini gastrin I Ac-LEEEEEAYGWMDF were obtained from Sigma Chemical Co. All the peptides were freeze-dried and dissolved in 50 mM Tris, 50 mM NaCl, pH 7.4, prior to use. Peptide annealing studies were performed by incubating the serpin at a final concentration of 1 mg/mL in 50 mM Tris, 50 mM NaCl, pH 8.0, with a 100-fold molar excess of peptide at 37 °C at the times indicated in each figure. The presence of binary complex was assessed by separating the proteins by 7.5–15% (w/v) nondenaturing PAGE.

Heat stability measurements and limited proteolysis of the engineered wild-type and S–S antitrypsins

Heat stability measurements were performed by heating both the recombinant wild-type and the S–S antitrypsins (0.4 mg/mL) in 20 mM Tris-HCl, pH 7.4, buffer at 60 °C, for the times indicated. Following incubation, the samples were cooled rapidly on ice and then mixed well prior to analysis by 7.5–15% (w/v) nondenaturing PAGE and electron microscopy. For cleavage studies, papain was incubated with the recombinant wild-type or S–S antitrypsin at enzyme:substrate (w:w) ratios of 1:250 and 1:100 in 30 mM potassium phosphate, 30 mM NaCl, pH 7.0, for 2 h at 37 °C. The reactions were terminated by the addition of SDS-polyacrylamide gel loading buffer (62.5 mM Tris, 3% w/v SDS, 10% v/v glycerol, pH 6.8) and heating at 100 °C for 2 min. Each sample was then divided into two equal volumes, one of which was made 100 mM with respect to DTT and incubated for 4 h at 23 °C before separating the proteins by 10–20% (w/v) SDS-PAGE.

Modeling of the loop-C-sheet polymerization mechanism

Modeling was done on a Silicon Graphics Indigo II workstation using the QUANTA/CHARMm interface (Molecular Simulations Inc., Cambridge, UK) unless otherwise stated.

The structures of intact ovalbumin (Stein et al., 1990) and cleaved antitrypsin (Loebermann et al., 1984) were obtained from the Protein Data Bank (Bernstein et al., 1977) and the structure of the antithrombin dimer was acquired from one of us (M.R.W.).

For modeling the loop-C-sheet polymerization mechanism, the native molecule obtained from the antithrombin dimer was first detached from part of its reactive loop by breaking the bonds at P'_1-P'_2 and P_9-P_8. This "clipped" molecule was then manipulated using dials relative to the latent molecule (and P_8-P'_1) using interactive graphics until there were no steric clashes (seen using distance constraints) and so that it was in an orientation that would require removal of s1C to link P'_2 to P'_1. The residues P'_1-P'_2 and P_9-P_8 were linked using a program developed by one of us (A.M.L.) to allow chain closure by means of a search in torsion angle space while constraining the deviations of the main-chain conformational angles from the initial value (Lesk, 1977). This resulted in the removal of s1C from the native molecule, making a dimer with a C-sheet available to receive another reactive loop. The dimer between the latent molecule and our modeled unit was then subjected to CHARMm minimization (with dihedral constraints applied to the reactive loop where necessary) until a satisfactory negative energy was reached.

To generate an antithrombin trimer, a copy of the partially inserted molecule (generated above) was linked onto a dimer (which has an open C-sheet) via the P_6-P_2 region of its reactive loop (using superimposition techniques to obtain the correct orientation of the new subunit). This trimer was also subjected to CHARMm minimization resulting in a satisfactory negative energy (−43,540 kcal/mol). Longer-chain models were built using α-carbon atoms only (because of atom number limitations in the program) and indicated that our model was capable of indefinite propagation without steric clashes.

Models of antitrypsin loop-C-sheet polymers were generated in a similar way. The model of the antithrombin dimer was first used as a template for homology modeling of the reactive loop of an antitrypsin monomer. However, in this case, the reactive loop was further inserted into the A-sheet to the P_{12} position. Also, because the antitrypsin reactive loop is shorter than that of antithrombin, the molecule was displaced using interactive graphics to a different orientation to allow chain closure between P'_1-P'_2 and P_9-P_8. The s1C of cleaved antitrypsin was used for homology modeling of the P_4-P_1 region in order to get the β-sheet hydrogen bond pattern in the C-sheet correct. The region binding to the C-sheet (P_5-P_1) is also different from that in antithrombin (P_6-P_2) in order to allow the proline at P_2 position to bind correctly to the β-sheet.

Modeling of the loop-A-sheet polymerization mechanism

The design for this mechanism of polymerization took into consideration the findings of Mast et al. (1992) that cleavage of antitrypsin at the P_9-P_8 or P_{10}-P_9 bonds results in spontaneous polymerization. This suggests that the P_{15}-P_9 region of one molecule inserts into the top of its own A-sheet leaving the bottom half of the A-sheet open and allowing the P_8-P_3 region of another molecule to insert subsequently, thereby forming the loop-A-sheet polymers. Cleaved antitrypsin was first superimposed onto fragment 1 of ovalbumin (Stein et al., 1990; Stein & Chothia, 1991) and homology modeling was used to model residues P_{16}-P_1 into the same form as ovalbu-

min. This produced antitrypsin molecule B (Fig. 6A), with the reactive loop fully exposed. Cleaved antitrypsin structure (molecule A of Fig. 6A) was used to homology-model residues P_8-P_1 of molecule B into the A-sheet of molecule A and then residues P_{16}-P_9 of molecule A were deleted temporarily. Molecule B was then related manually to molecule A using interactive graphics until residues P_9 and P_1' were in reasonable proximity to residues P_8 and P_1 without steric clashes between the two monomers. The chain closure program was used to close the gaps between P_9-P_8 and P_1-P_1' and the model subjected to CHARMm minimization with dihedral constraints. This resulted in an antitrypsin dimer consisting of one antitrypsin molecule (B) with its reactive loop totally expelled from the A-sheet and residues P_8-P_3 inserted into the A-sheet of another molecule (A). Molecule A was then replaced with a copy of molecule B. The relative position of the two monomers was then adjusted for further loop-A-sheet polymerization. During this process, it was found necessary to displace s1C from the C-sheet to facilitate the propagation of the long-chain polymers without steric clashes. As with the loop-C-sheet polymerization model, the ϕ, ψ, and ω angles of the reactive loop were checked and the polymer subjected to full CHARMm minimization until the CHARMm energy reached a stable low value. The same modeling method was also used to generate the antithrombin loop-A-sheet polymers, but, in this case, the L-antithrombin was used as the basis of the monomer and, as a consequence, s1C was modeled by using native antithrombin as a template. As described above, ovalbumin was used to model the turn at the top of the A-sheet (Stein et al., 1990; Stein & Chothia, 1991).

Acknowledgments

We thank Dr. John T. Finch, Laboratory of Molecular Biology, MRC Centre, Cambridge, for the electron micrographs, and Dr. Len C. Packman, Department of Biochemistry, University of Cambridge, for peptide synthesis, amino acid analysis, and N-terminal sequence analysis. This work was supported by the British Heart Foundation, the European Community grant BMH1-CT93-1592, and the Wellcome Trust.

References

Aulak KS, Eldering E, Hack CE, Lubbers YPT, Harrison RA, Mast A, Cicardi M, Davis AE. 1993. A hinge region mutation in C1-inhibitor ($Ala^{436} \rightarrow Thr$) results in nonsubstrate-like behavior and in polymerization of the molecule. *J Biol Chem 268*:18088–18094.

Baumann U, Bode W, Huber R, Travis J, Potempa J. 1992. Crystal structure of cleaved equine leukocyte elastase inhibitor determined at 1.95 Å resolution. *J Mol Biol 226*:1207–1218.

Baumann U, Huber R, Bode W, Grosse D, Lesjak M, Laurell CB. 1991. Crystal structure of cleaved human α_1-antichymotrypsin at 2.7 Å resolution and its comparison with other serpins. *J Mol Biol 218*:595–606.

Bernstein FC, Koetzle TF, Williams GJB, Meyer EF Jr, Brice MD, Rodgers JR, Kennard O, Simanouchi T, Tasumi M. 1977. The Protein Data Bank: A computer-based archival file for macromolecular structures. *J Mol Biol 112*:535–542.

Björk I, Ylinenjärvi K, Olson ST, Bock PE. 1992. Conversion of antithrombin from an inhibitor of thrombin to a substrate with reduced heparin affinity and enhanced conformational stability by binding of a tetradecapeptide corresponding to the P_1 to P_{14} region of the putative reactive bond loop of the inhibitor. *J Biol Chem 267*:1976–1982.

Bruce D, Perry DJ, Borg JY, Carrell RW, Wardell MR. 1994. Thromboembolic disease due to thermolabile conformational changes of antithrombin Rouen-VI ($^{187}Asn \rightarrow Asp$). *J Clin Invest 94*:2265–2274.

Carrell RW, Stein PE, Fermi G, Wardell MR. 1994. Biological implications of a 3 Å structure of dimeric antithrombin. *Structure 2*:257–270.

Chang WSW, Wardell MR, Lomas DA, Carrell RW. 1996. Probing serpin reactive-loop conformations by proteolytic cleavage. *Biochem J 314*:647–653.

Eldering E, Verpy E, Roem D, Meo T, Tosi M. 1995. COOH-terminal substitutions in the serpin C1-inhibitor that cause loop overinsertion and subsequent multimerization. *J Biol Chem 270*:2579–2587.

Elliott PR, Lomas DA, Carrell RW, Abrahams JP. 1996. Inhibitory conformation of the reactive loop of α_1-antitrypsin. *Nature Struct Biol 3*:676–681.

Ellman GL. 1959. Tissue sulfhydryl groups. *Arch Biochem Biophys 82*:70–77.

Faber JP, Poller W, Olek K, Baumann U, Carlson J, Lindmark B, Eriksson S. 1993. The molecular basis of α_1-antichymotrypsin deficiency in a heterozygote with liver and lung disease. *J Hepatol 18*:313–321.

Gettins P, Patston PA, Schapira M. 1993. The role of conformational change in serpin structure and function. *BioEssays 15*:461–467.

Goldenberg DP. 1989. Analysis of protein conformation by gel electrophoresis. In: Creighton TE, ed. *Protein structure: A practical approach*. Oxford: IRL Press. pp 225–250.

Hopkins PCR, Stone SR. 1995. The contribution of the conserved hinge region residues of α_1-antitrypsin to its reaction with elastase. *Biochemistry 34*:15872–15879.

Huber R, Carrell RW. 1989. Implications of the three-dimensional structure of α_1-antitrypsin for structure and function of serpins. *Biochemistry 28*:8951–8966.

Koloczek H, Banbula A, Salvesen G, Potempa J. 1996. Probing the shape of α_1-proteinase inhibitor conformers by intrinsic fluorescence. *The International Symposium on the Chemistry and Biology of Serpins*:111. [Abstr.]

Laemmli UK. 1970. Cleavage of structural proteins during the assembly of the head of bacteriophage T4. *Nature 227*:680–685.

Lesk AM. 1977. Macromolecular marionettes. *Comput Biol Med 7*:113–129.

Loebermann H, Tokuoka R, Deisenhofer J, Huber R. 1984. Human α_1-proteinase inhibitor: Crystal structure analysis of two crystal modifications, molecular model and preliminary analysis of the implications for function. *J Mol Biol 177*:531–556.

Lomas DA, Elliott PR, Sidhar SK, Foreman RC, Finch JT, Cox DW, Whisstock JC, Carrell RW. 1995. $Alpha_1$-antitrypsin M_{malton} (Phe^{52}-deleted) forms loop-sheet polymers in vivo: Evidence for the C sheet mechanism of polymerization. *J Biol Chem 270*:16864–16870.

Lomas DA, Evans DL, Finch JT, Carrell RW. 1992. The mechanism of Z α_1-antitrypsin accumulation in the liver. *Nature 357*:605–607.

Lomas DA, Evans DL, Stone SR, Chang WSW, Carrell RW. 1993a. Effect of the Z mutation on the physical and inhibitory properties of α_1-antitrypsin. *Biochemistry 32*:500–508.

Lomas DA, Finch JT, Seyama K, Nukiwa T, Carrell RW. 1993b. $Alpha_1$-antitrypsin S_{iiyama} ($Ser^{53} \rightarrow Phe$): Further evidence for intracellular loop-sheet polymerization. *J Biol Chem 268*:15333–15335.

Mast AE, Enghild JJ, Salvesen G. 1992. Conformation of the reactive site loop of α_1-proteinase inhibitor probed by limited proteolysis. *Biochemistry 31*:2720–2728.

McKay EJ. 1981. A simple two-step procedure for the isolation of antithrombin III from biological fluids. *Thromb Res 21*:375–382.

Mikus P, Urano T, Liljestrom P, Ny T. 1993. Plasminogen activator inhibitor 2 (PAI-2) is a spontaneously polymerizing serpin: Biochemical characterization of the recombinant intracellular and extracellular forms. *Eur J Biochem 218*:1071–1082.

Mourey L, Samama JP, Delarue M, Petitou M, Choay J, Moras D. 1993. Crystal structure of cleaved bovine antithrombin III at 3.2 Å resolution. *J Mol Biol 232*:223–241.

Nordenman B, Nyström C, Björk I. 1977. The size and shape of human and bovine antithrombin III. *Eur J Biochem 78*:195–203.

Patston PA, Hauert J, Michaud M, Schapira M. 1995. Formation and properties of C1-inhibitor polymers. *FEBS Lett 36*:401–404.

Potempa J, Korzus E, Travis J. 1994. The serpin superfamily of proteinase inhibitors: Structure, function, and regulation. *J Biol Chem 269*:15957–15960.

Schechter I, Berger A. 1967. On the size of the active site in proteases. 1. Papain. *Biochem Biophys Res Commun 27*:157–162.

Schulze AJ, Baumann U, Knof S, Jaeger E, Huber R, Laurell CB. 1990. Structural transition of α_1-antitrypsin by a peptide sequentially similar to β-strand s4A. *Eur J Biochem 194*:51–56.

Stein PE, Carrell RW. 1995. What do dysfunctional serpins tell us about molecular mobility and disease? *Nature Struct Biol 2*:96–113.

Stein PE, Chothia C. 1991. Serpin tertiary structure transformation. *J Mol Biol 221*:615–621.

Stein PE, Leslie AGW, Finch JT, Turnell WG, McLaughlin PJ, Carrell RW. 1990. Crystal-structure of ovalbumin as a model for the reactive center of serpins. *Nature 347*:99–102.

Travis J, Johnson D. 1981. Human α_1-proteinase inhibitor. *Methods Enzymol 80*:754–765.

Travis J, Salvesen G. 1983. Human plasma proteinase inhibitors. *Annu Rev Biochem 52*:655–709.

Wu Y, Foreman RC. 1990. The effect of amino acid substitutions at position 342 on the secretion of human α_1-antitrypsin from *Xenopus* oocytes. *FEBS Lett 268*:21–23.